J Mol Model (2001) 7:392–397
DOI 10.1007/s00894-001-0056-7

ORIGINAL PAPER

Tarek M. Madkour · Abdel H. Ebaid

Intrinsic atomic-level forces in polymer networks exhibiting non-gaussian effects: relationship with the limited chain extensibility

Received: 19 June 2001 / Accepted: 1 October 2001 / Published online: 14 November 2001

Abstract Intrinsic atomic-level forces for networks exhibiting non-Gaussian effects were evaluated during the integration of the equations of motion using the Verlet algorithm. The forces acting on the junction points of the cross-linking chains and the elastomeric chains of unimodal and bimodal network arrangements showed no apparent change as a consequence of the network variation. The forces acting on the short chains in a bimodal network cross-linked using sulfur atoms and relatively long polyquinone chains had much higher values than those in a unimodal network arrangement. Nevertheless, the intrinsic forces acting on the polyquinone atoms decreased dramatically as a result of the formation of bimodal networks. The presence of relatively long polyquinone chains in bimodal networks caused the short sulfur chains to stretch to their maximum extensibility and they can no longer increase their end-to-end separation by simple rotations about their skeletal bonds. Limited chain extensibility of the short chains resulting from the deformation of the bond angles and bond lengths led to much higher potential energies, as determined using the dynamic quenching technique. This resulted in the non-Gaussian effects known for bimodal networks and their subsequent anomalous mechanical properties. The dynamical behavior of the nuclei bending and torsional angles was also investigated for the unimodal and bimodal networks.

Keywords Intrinsic atomic-level forces · Non-Gaussian effects · Bimodal chain length distribution · Limited chain extensibility · Nuclei bending and torsional angles

T.M. Madkour (✉) · A.H. Ebaid
Department of Chemistry, Helwan University, Ain-Helwan, Cairo, Egypt 11795
e-mail: drmadkour@yahoo.com

Introduction

Polymer networks cured with two different vulcanizing agents of different lengths exhibit non-Gaussian effects that are synonymous for either bimodal networks or networks that can undergo a strain-induced crystallization. [1, 2] Sharaf and Mark [3] theoretically investigated elastomeric networks with two cross-linking systems, namely, very short sulfur cures and sufficiently long polysulfidic cross-links, which were then assumed to be elastically effective and would thus contribute to the modulus of the samples by increasing their end-to-end distances and decreasing their entropies in response to the imposed stress. Eventually, this will lead to the superior mechanical properties that bimodal networks are known to possess. [4, 5, 6, 7] The increase in the modulus and the anomalous improvements in the ultimate properties of the bimodal networks are thought to be due to intramolecular effects, specifically to non-Gaussian effects arising from the limited chain extensibility. The hypothesis as outlined by Curro and Mark [8] states that a network chain near its maximum extensibility can no longer increase its end-to-end separation by configurational changes, i.e., by simple rotations about its skeletal bonds. Deformations of bond angles (and possibly even bond lengths) would be required, and the energies for those processes are much greater than those for configurational changes. The forces, acting microscopically, on the individual long and short network chains could be evaluated by considering a bimodal network consisting of N_S short chains and N_L long chains. The free energy change $\Delta A(\alpha)$ due to the deformation of the network long (L) chains and short (S) chains with a uniaxial stretch ratio (α) is given by:

$$\Delta A(a) = \Delta A_L(a_L) + \Delta A_S(a_S) \quad (1)$$

Making use of the conventional rubber-like elasticity theory, [9] the free energy change of the long chains is given by:

$$\Delta A_L = KTN_L/2V\left(a_L^2 + 2/a_L - 3\right) \quad (2)$$

whereas the free energy change of the short chains is given by: [10]

$$\Delta A_S = N_S/3V \left[A_o(r_o a_S) + 2A_o\left(r_o a_S^{-1/2}\right) - 3A_o(r_o)\right] \quad (3)$$

where r_o is the root-mean-squared value of the end-to-end distance. The intrinsic microscopic deformation could be thus related to the macroscopic deformation by (i) considering the average microscopic deformation to be affine,

$$\alpha = x_L \alpha_L + x_S \alpha_S \quad (4)$$

$$(\partial \Delta A/\partial \alpha_S)_\alpha = 0 \quad (5)$$

Applying the extreme condition in Eq. (5) into Eqs. (1)–(4) yields the relationship:

$$r_o/3 \left[A'_o(r_o a_S) - a_S^{-3/2} A'_o\left(r_o a_S^{-1/2}\right)\right] = KT/x_L \left[(a - a_S x_S) - x_L^3 (a - a_S x_S)^{-2}\right] \quad (6)$$

The nominal force, f*, on the network can be obtained from the following considerations:

$$f* = KT(\partial A/\partial \alpha) = KT[(\partial A/\partial \alpha)_{\alpha S} + (\partial S/\partial \alpha_S)_\alpha \partial \alpha_S/\partial \alpha] \quad (7)$$

The second term on the right-hand side of Eq. (7) vanishes in view of Eq. (6), and thus we obtain:

$$f* = -KT(\partial A/\partial \alpha)_{\alpha S} \quad (8)$$

and finally,

$$f* = vKT\left[\alpha/x_L - x_S \alpha_S/x_L - (\alpha/x_L - x_S \alpha_S/x_L)^{-2}\right] \quad (9)$$

thus implying the relationship between the microscopic deformation of the individual short chains and the macroscopic deformation, α, which is well described by the virial stress formula, [11] where the macroscopic stress tensor in a polymer system may be expressed as a sum of the intrinsic atomic-level stress tensors, with each of the latter associated with a single atom.

Recently, [12] we showed that the incorporation of the polymerization products of *p*-benzoquinone into a sulfur-cured matrix such as styrene–butadiene rubber (SBR) had a profound effect on the mechanical properties of the elastomeric networks, which was explained on the basis of the formation of bimodal networks. The polyquinone chains consist of a series of either benzenoid (HQ) or quinonoid (BQ) nuclei or both (AQ). These nuclei are planar in nature and changes about the bond angles or the torsional angles within the single nuclei are highly unlikely. The only types of motion these materials might perform must involve bonds connecting the different nuclei. Torsion and/or quinonoid–benzenoid nuclei bending about the connecting bonds are such examples. Nevertheless, the polymeric materials are expected to behave differently in terms of their chemical natures. [13] It is expected that hydrogen bonding developed in polyquinone, polybenzoquinone and polyhydroquinone would have a significant role on their dynamics.

In this article, we focus on the behavior of bimodal networks cured using two different cross-linking systems such as sulfur and the polymerization products of *p*-benzoquinone. We examine the three forms of polyquinone, the fully oxidized form, polybenzoquinone (BQ), the fully reduced form, polyhydroquinone (HQ), and polyquinone (AQ), which consists of both benzenoid and quinonoid nuclei. We also examine the intrinsic atomic-level forces (f_i) acting on the junction atoms, where the cross-linking agents are attached to the elastomeric chains, on the sulfur atoms connecting the elastomeric chains and on the polyquinone atoms comprising the second cross-linking agent of the longer chains. The study is also extended to investigate the dynamics of the polyquinone chains through which the various polyquinone forms may decrease their entropies in response to the imposed stress.

Methodology

The intrinsic forces acting on the various atoms comprising a cross-linked system are normally evaluated during the integration of the classical equations of motion. For a system of atoms, with Cartesian coordinates $\mathbf{r}_i$ and mass of atom m_i, the force exerted on that atom is given by:

$$m_i \cdot \ddot{\mathbf{r}}_i = \mathbf{f}_i \quad (10)$$

where $\ddot{\mathbf{r}}$ is the second derivative of $\mathbf{r}_i$ with respect to the time t. The force acting on atom i is related to the potential energy exerted on atom i, V, by:

$$\mathbf{f}_i = -\nabla_{\mathbf{r}i} V \quad (11)$$

Integration of the equation of motion during a dynamics run is usually achieved by the evaluation of the total potential energy exerted on atom i and the calculation of the force $\mathbf{f}_i$ acting on this atom accordingly. This is done by evaluating all pairwise potentials between atom i and all other atoms in the system within a loop over all pairs of i and j atoms. The pairwise potential energy, $V(\mathbf{r}_{ij})$, the pair virial function, $W(\mathbf{r}_{ij})$, and the pairwise force directed along the interatomic vector, $\mathbf{r}_{ij}$, are all related according to: [13]

$$f_{ij} = -\frac{1}{r_{ij}}\left(\frac{dV(r_{ij})}{d_{r_{ij}}}\right) r_{ij} = \frac{W(r_{ij})}{r_{ij}^2} r_{ij} \quad (12)$$

Insight II software module employing the COMPASS [14] force-field was used to perform the dynamics simulation. The COMPASS force-field is a class III force-field constructed using exact ab initio quantum mechanics calculations and well-validated against most organic and inorganic type of interactions. Periodic boundary conditions enable simulations to be carried out on relatively small molecular systems, in such a way that the atoms experience forces as if they were in the bulk phase. The system is represented by a small number of atoms contained within a periodic cell that is replicated in three dimensions. The amorphous cells of the various systems

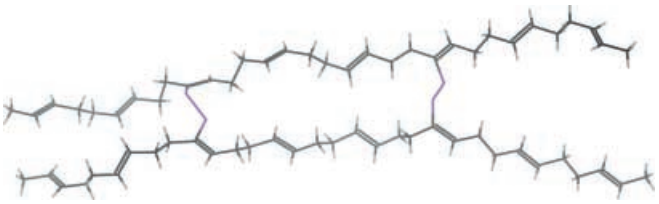

Fig. 1 Graphical representation of a unimodal polybutadiene network cross-linked using only sulfur atoms

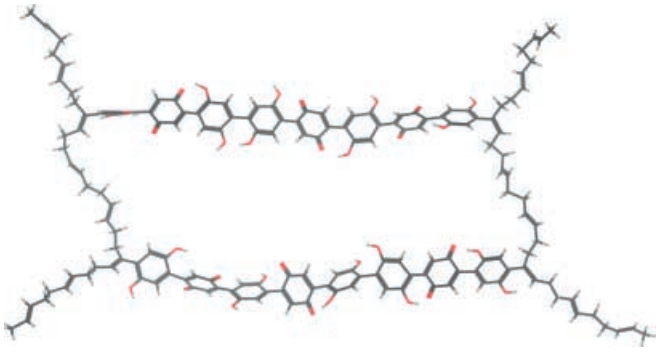

Fig. 2 Graphical representation of a unimodal polybutadiene network cross-linked using polyquinone chains (AQ)

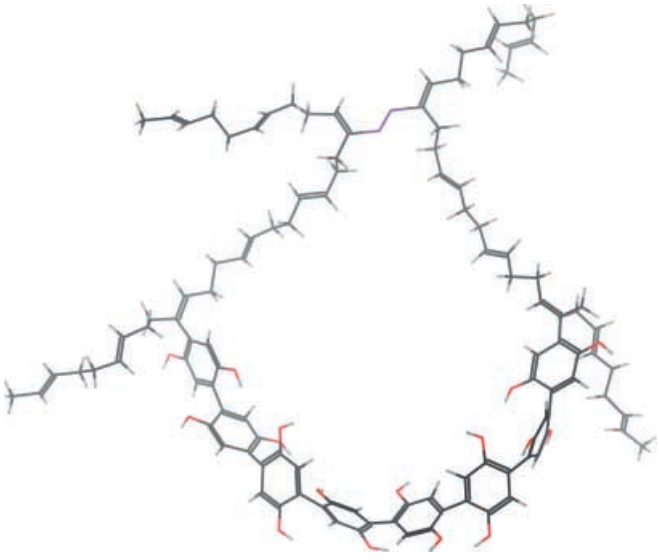

Fig. 3 Graphical representation of a bimodal polybutadiene network cross-linked using sulfur atoms and polyhydroquinone long chains

were built using two cross-linked polybutadiene chain conformations, each consisting of five repeat units. Figures 1, 2 and 3 illustrate graphical representations of three of the cross-linked systems that were under study. The system shown in the first figure is sulfur cross-linked polybutadiene elastomeric chains. The system in the second figure represents a unimodal cross-linked polybutadiene elastomer. The cross-linking system in this case is polyquinone chains. The third figure illustrates a bimodal cross-linked polybutadiene elastomer cross-linked using short sulfur chains and relatively long polyhydroquinone chains. A total of seven systems were under study, namely, four unimodal systems cross-linked using sulfur, polyquinone (AQ), polybenzoquinone (BQ), and polyhydroquinone (HQ), respectively, as well as three bimodal cross-linked systems, which were all cross-linked using two different cross-linking agents. Of those two cross-linking agents the short chains were composed of only two sulfur atoms. The second cross-linking system is chosen to be AQ, BQ or HQ of a variable segment length, L_{seg}, in the range of three to ten units. This was done in order to investigate the effect of the chain length of the long cross-linking agent on the forces exerted on the elastomeric atoms.

After equilibration and minimization, the cross-linked systems were then grown within a cubic box at room temperature using a traditional rotational isomeric states (RIS) method. The volume of all the simulated boxes was chosen to correspond to the experimental density of a cross-linked polybutadiene. In order to account for all of the long-range interactions, the Ewald summation method was used so as to allow a charged particle to interact with all other particles in the simulation cell and with all of their images in an infinite array of periodic cells. After minimization and equilibration, molecular dynamics runs took place at the vicinity of room temperature for 1 ns using the NVT ensemble, which was followed by another 1 ns using the NPT ensemble. An external hydrostatic pressure of magnitude 1 MPa was then applied to the simulated boxes to represent the negative isotropic component of a normal stress tensor. The molecular dynamics procedures were then allowed to progress under the stress applied for another 5 ns. At the end of every run, a trajectory file was stored for later analysis of the intrinsic atomic forces exerted on the various atoms. Four runs were performed for every particular experiment for better averaging. Error bars shown in all the figures refer to the standard errors.

Results and discussion

Energy minimization of the various unimodal and bimodal cross-linked systems was performed using the dynamic quenching method. [15] The technique involves coupling the system to a thermal bath to allow for temperature variation. This is simulated by constantly monitoring and adjusting the average kinetic energy of the atoms to maintain a newly given temperature during a molecular dynamics run. By setting the target temperature to a very low value (e.g. 1 K) the system overcomes small barriers during the relaxation procedure to finally settle in a lower-energy minimum. The total potential energies of the minimized structures are shown in Table 1. The higher potential energies of the bimodal networks as compared to the unimodal ones are due to the intramolecular effects arising from the presence of the bimodal cross-linking. Since a network chain near its maximum extensibility can no longer in-

Table 1 Potential energies of the various systems having unimodal and bimodal cross linking arrangements of the three chemically different polymerization products of *p*-benzoquinone studied using energy minimization techniques

Segment length	Total potential energy (kcal mol^{-1})					
	Unimodal cross-linking			Bimodal cross-linking		
	AQ	BQ	HQ	AQ	BQ	HQ
3	75.4	176.7	244.2	112.3	282.7	476.0
4	95.9	207.2	367.8	119.5	336.2	651.2
5	99.6	247.1	509.7	146.5	391.7	863.8
6	102.9	270.3	577.1	195.6	467.8	1075.0
7	139.7	323.2	697.4	208.1	517.0	1241.9
8	140.6	339.1	776.0	217.9	606.6	1547.7
9	169.8	357.2	887.4	246.8	698.4	1669.8
10	183.7	375.6	998.0	270.1	794.3	1891.1

Table 2 Intrinsic atomic-level forces acting on the junction atoms of the cross-linking systems and the elastomeric chains of different unimodal and bimodal arrangements

Segment length	Intrinsic forces (kcal mol^{-1} Å^{-1})					
	Unimodal cross-linking			Bimodal cross-linking		
	AQ	BQ	HQ	AQ	BQ	HQ
3	38.34	40.24	37.56	39.30	39.14	41.17
4	38.69	35.30	39.34	40.06	40.38	39.77
5	37.08	38.27	37.51	38.71	41.28	39.29
6	37.48	39.38	39.66	38.58	40.56	40.66
7	40.23	37.23	39.79	37.94	40.18	39.78
8	37.96	38.17	37.60	39.84	39.92	38.92
9	40.15	37.14	38.61	40.80	40.37	40.30
10	36.26	40.63	37.55	39.48	39.37	40.11

crease its end-to-end separation by simple rotations about the skeletal bonds, deformation of the bond angles and lengths leading to greater potential energy values would be required. Furthermore, potential energy results show that polyquinone networks (AQ) are greatly stabilized by the presence of the hydrogen bonding between the hydroxyl hydrogen attached to the benzenoid rings and the carbonyl oxygens of the quinonoid ones. Increasing the segment length of the polyquinone chains also resulted in an increase of the total potential energies of these systems.

Values for the intrinsic atomic-level forces acting on the junction atoms of the cross-linking systems and the elastomeric chains are listed in Table 2. The table clearly shows that these forces have practically similar values irrespective of the type, arrangement or the segment length of the cross-linking agents within the statistical errors. This indicates, however, that the various arrangements of the cross-linking agents do not influence the elastomeric chains but rather affect intrinsically the cross-linking chains themselves. Figure 4 represents the intrinsic forces acting on the sulfur atoms making up the short chains in bimodal network arrangements. All data in this figure represent the forces on the sulfur atoms, whereas the legend of the figure refers to the type of the second cross-linking agent. The figure clearly shows that for a network cross-linked using sulfur atoms only, Fig. 1, the forces acting on these sulfur atoms had the lowest values. Replacement of one of the sulfur short chains by a relatively long polyquinone chain caused the stress on the other sulfur short

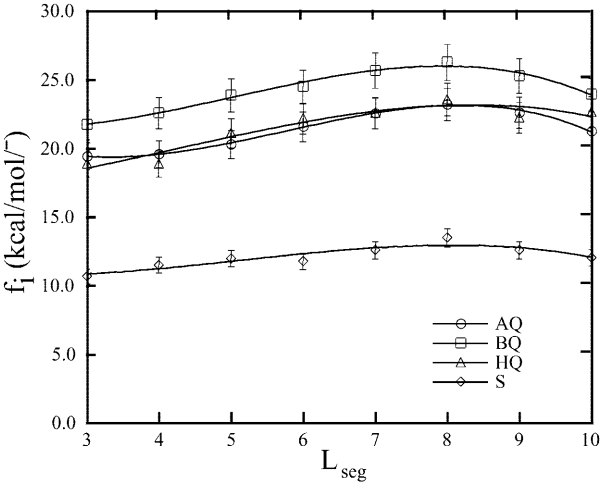

Fig. 4 Intrinsic atomic-level forces acting on the sulfur atoms in bimodal network arrangements. See text

chain to increase dramatically, possibly due to the limited chain extensibility of these short chains, Fig. 3. To clarify this further, the forces on the polyquinone atoms in unimodal and bimodal arrangements were evaluated and plotted in Figs. 5 and 6, respectively. Comparison of the two figures indicates that the intrinsic forces acting on the polyquinone atoms decreased as a result of the formation of bimodal networks and the limited chain extensibility of the short sulfur chains. Figures 4, 5 and 6 also show that,

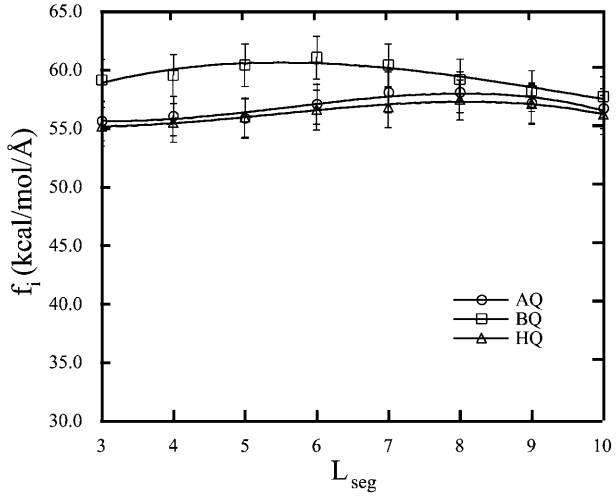

Fig. 5 Intrinsic atomic-level forces acting on the various atoms making up the polyquinone cross-linking chains in unimodal network arrangements

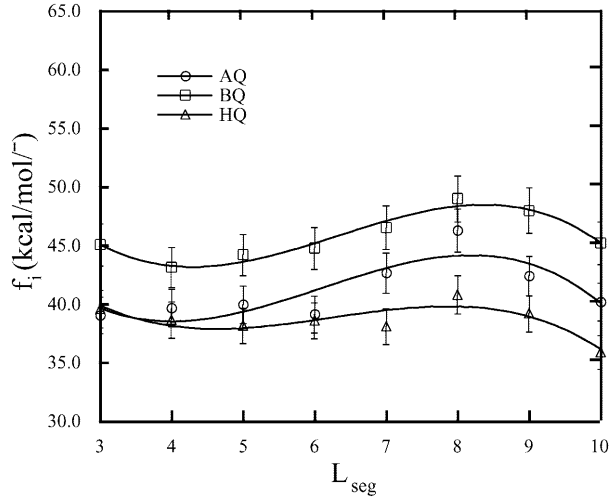

Fig. 6 Intrinsic atomic-level forces acting on the various atoms making up the polyquinone cross-linking chains in bimodal network arrangements

for the three chemically different polyquinone chains, polybenzoquinone-cross-linked networks had the highest stress values. This is possibly due to the absence of any hydrogen bonding formation in these chains. To elaborate further on this observation, the dynamics of the three-polyquinone chain types were also investigated.

For polyquinone chains, torsions of four-body systems as well as bending of three-body systems within the various nuclei constituting the chains are highly unlikely. Therefore, only changes about the skeletal bonds connecting the different nuclei are considered. Two primary factors are of interest here, the bending and the torsion of the consecutive nuclei with respect to each other. Figure 7 shows a schematic drawing of the two angles under consideration. The nuclei bending angle (θ) is the angle between the two vectors connecting the carbon atoms of each nucleus in the *para* position with respect to the carbon atoms of the bond connecting the two nuclei. The nuclei torsional angle (ϕ) is the dihedral angle defined by the four atoms about the bond connecting the two nuclei. Figures 8 and 9 represent the average nuclei bending an-

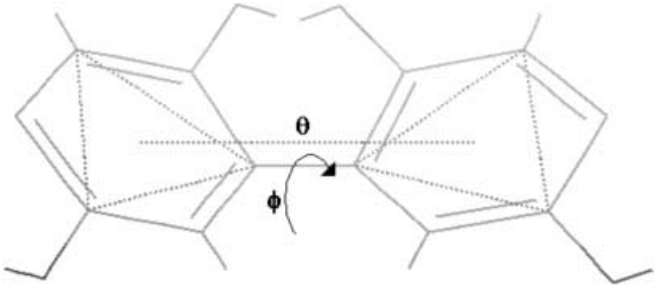

Fig. 7 Schematic drawing representing the nuclei bending angle (θ) and the nuclei torsional angle (ϕ)

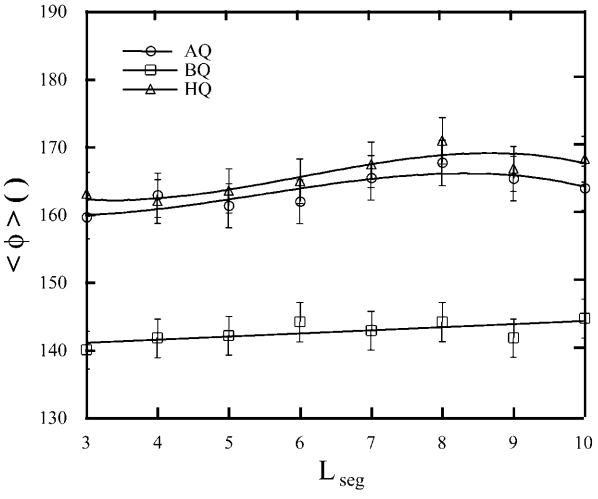

Fig. 8 The dependence of the average bending angle (< θ >) of various unimodal systems on the segment length of the polyquinone chains

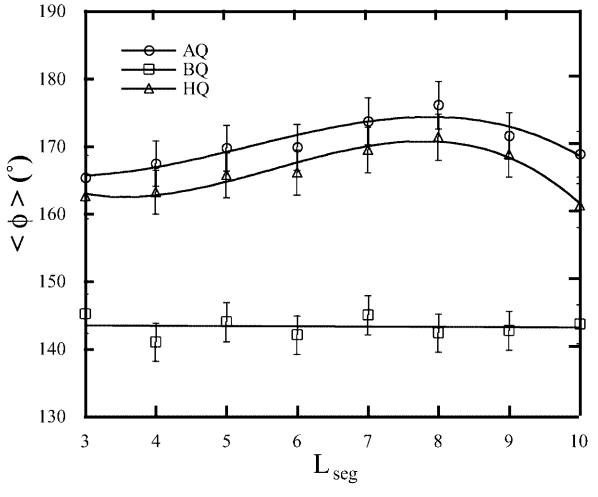

Fig. 9 The dependence of the average bending angle (< θ >) of various bimodal systems on the segment length of the polyquinone chains

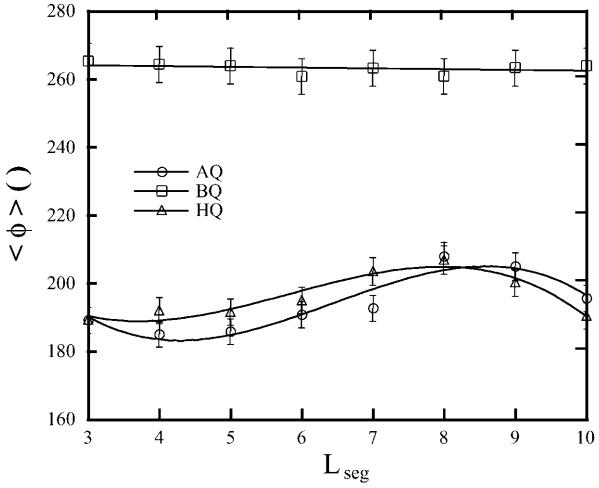

Fig. 10 The dependence of the average torsional angle (< ϕ >) of various unimodal systems on the segment length of the polyquinone chains

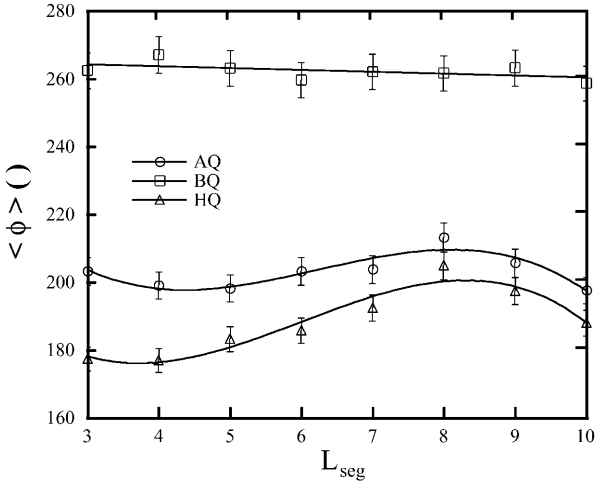

Fig. 11 The dependence of the average torsional angle (< ϕ >) of various bimodal systems on the segment length of the polyquinone chains

gles of the different polyquinone chains as a function of the segment length of the polyquinone chain in unimodal and bimodal network arrangements, respectively. Polyquinone (AQ) and polyhydroquinone (HQ) being mostly stabilized by hydrogen bonding show similar nuclei bending behavior. The presence of the hydrogen bonds between the hydroxyl groups on neighbouring hydroquinone nuclei should restrict to some extent the torsional movement of these nuclei about the bonds connecting them. Figures 10 and 11 represent the average torsional angle of the three-polyquinone systems as a function of the segment length of the polyquinone chain in unimodal and bimodal network arrangements, respectively. The figures indicate the easiness of the torsional movement of polybenzoquinone, possibly due to the lack of any hydrogen bonding between the neighbouring nuclei. However, it should be noted that the torsion in polybenzoquinone chains must also be somewhat restricted. This is because of the partial negative charges the carbonyl oxygen atoms may carry. The maximum repulsion between these charged atoms must therefore take place as the torsional angles approach 180°, with the highest points of the energy barriers at this angle. These barriers must therefore be high enough not to be easily overcome and only fluctuations between these barriers must therefore be allowed.

Conclusion

Non-Gaussian effects synonymous with polymer networks cross-linked using two different vulcanizing agents of different lengths are known to result from the limited chain extensibility of the short chains present in the network. The short chains near their maximum extensibility can no longer increase their end-to-end separation by simple rotations about their skeletal bonds. Therefore deformation of the bond angles and bond lengths of the short chains will be required in response to the imposed stress. These deformations demand greater energies than those for the configurational changes. Intrinsic atomic-level forces evaluated for the various atoms in the polymer networks of unimodal and bimodal chain length distribution indicated that the atoms at the junction points of the cross-linking agents and the elastomeric chains suffer no extra stress due to the change in the network chain length distribution. The intrinsic forces acting on the atoms making up the short chains increase dramatically upon the formation of the bimodal networks at the expense of the stress values acting on the long chains. The limited chain extensibility, in this case, has acted so as to increase the total potential energy of these networks and consequently their nominal force, giving rise to the anomalous modulus values that bimodal networks are known to have.

References

1. Sabaa MW, Madkour TM, Yassin AA (1988) Polym Degrad Stab 22:205
2. Hagn C, Wittkop M, Kreitmeier S, Trautenberg HL, Holzl T, Goritz D (1997) Polym Gels Networks 5:327
3. Sharaf MA, Mark JE (1991) Macromol Rep A 28:67
4. Queslel JP, Mark JE (1986) Encycl Polym Sci Technol 5:365
5. Madkour TM, Mark JE (1994) Macromol Rep A 3:153
6. Galiatsatos V, Mark JE (1987) Macromolecules 20:4521
7. von Lockette PR, Arruda EM (1999) Macromolecules 32:1990
8. Curro JG, Mark JE (1984) J Chem Phys 80:4521
9. Treloar LEG (1975) The physics of rubber elasticity, 3rd edn. Clarendon Press, Oxford
10. Mark JE, Curro JG (1983) J Chem Phys 79:5705
11. Gao J, Weiner JH (1989) J Chem Phys 90:6749
12. Madkour TM, Hamdi MS (1996) J Appl Polym Sci 61:1239
13. Allen MP, Tildesley DJ (1987) Computer simulation of liquids. Clarendon Press, Oxford
14. Rigby D, Sun H, Eichinger BE (1997) Polym Int 44:311
15. Berendsen HJC, Postma JPM, van Gunsteren WF, DiNola A, Haak JR (1984) J Chem Phys 81:3684